

CENTRAL CATADIOPTRIC CAMERA CALIBRATION WITH SINGLE IMAGE*

Lei Zhang¹, Xin Du¹, Yunfang Zhu², Jilin Liu¹

1. Department of Information Science and Electronic Engineering,
Zhejiang University, Hangzhou, China

2. College of Computer and Information Engineering,
Zhejiang Gongshang University, Hangzhou, China
duxin@zju.edu.cn

ABSTRACT

Central catadioptric camera is a class of omnidirectional sensor having single effective viewpoint with reflective surfaces and lenses. This work studies the geometry of central catadioptric projection of a set of lines and adopts it into calibration. In this paper, we propose a practical calibration method for central catadioptric cameras by manually labeling the corners on planar grids. This method analytically parameterizes the intersection of a set of lines, regardless whether they are parallel or not. Algebraic distance is introduced in order to robustify this method since the conic which is the projection of line, is difficult to be obtained precisely. Moreover, it is proved that central catadioptric is able to calibrate by at least one image with two lines. The performance of this method is validated by both simulation data and real image data.

Index Terms— Catadioptric, intersection, calibration

1. INTRODUCTION

A camera with large field of view is required in many applications, such as robot navigation, surveillance, model acquisition for virtual reality. Combining traditional camera with mirrors, referred to as catadioptric camera, is one of the effective ways to enhance the sensor's field of view. During the last decade, there has been a considerable effort in designing and studying catadioptric cameras. Entire class of catadioptric cameras can be simply classified into central and non-central imaging systems, depending on whether they pose a single viewpoint [1] [8]. A unifying model was proposed for central catadioptric imaging system [5].

Previous work specifically on central catadioptric camera calibration can be divided into three different categories. The first category exploited prior knowledge about the scene, such as planar grids. An assumption was made that the projection function can be described by a Taylor series expansion [6]. The second category made use of the correspondences among multiple views for self-calibration [9]. The third category used properties of lines without any metric information. In [7], it was announced that a line in 3D space was mapped into a conic by central catadioptric cameras, where the information of unifying model was encoded in conics. Barreto and Araujo reported algorithms that located both the effective viewpoint and the absolute conic in the catadioptric image plane from the images of three lines [2], [3]. Furthermore, sphere images were introduced for calibration [10].

In this paper we focus on the central catadioptric cameras and propose a novel calibration algorithm on the basis of geometric

properties of lines. We exploit planar grids with known control points that are widely used in conventional camera calibration. Previous methods usually consider entities separately, which inspires us to introduce a common constraint of lines involved in some relationships into calibration. Moreover, the proposed method is able to calibrate by at least one image with 2 lines containing 6 points per line. Decrease in the number of lines evidently reduces the workload of manually labeling for researchers.

2. THE UNIFYING THEORY FOR CENTRAL CATADIOPTRIC CAMERA

In [5], Geyer and Daniilidis proved the equivalence of the central catadioptric projection and the composition of a two-step projection through a unit sphere, depicted in Figure 1. The unit sphere centers at origin, coincident with focus of reflective surface, which is also the origin of the world coordinate. Given an arbitrary point $\mathbf{X} = (X, Y, Z, 1)^T$ in homogeneous coordinate. \mathbf{X} is projected onto the unit sphere as

$$\mathbf{X}_s = \left(\frac{X}{r}, \frac{Y}{r}, \frac{Z}{r}, 1 \right)^T, \text{ where } r = \sqrt{X^2 + Y^2 + Z^2}.$$

Then, point \mathbf{X}_s on the unit sphere is projected from point \mathbf{O}_c to $\mathbf{x} = (x, y, 1)^T$ on a metric plane Π_m , by perspective transformation

$$\mathbf{P} = \begin{pmatrix} f_e & 0 & 0 & 0 \\ 0 & f_e & 0 & 0 \\ 0 & 0 & 1 & l \end{pmatrix}, \text{ where } l = |OO_c| \text{ and } f_e = |O_c O_p|.$$

An affine transformation

$$\mathbf{K} = \begin{pmatrix} r & s & u_0 \\ 0 & 1 & v_0 \\ 0 & 0 & 1 \end{pmatrix}$$

projects point \mathbf{x} to point $\mathbf{m} = (u, v, 1)^T$ on image plane Π_M . Combining \mathbf{P} and \mathbf{K} , we obtain the camera matrix of the virtual camera $\mathbf{P}_{virtual} = \mathbf{K}\mathbf{P}$.

In general, five intrinsic parameters for the virtual camera can be distinguished including aspect ratio r , skew factor s , principal point $\mathbf{O}_p (u_0, v_0)$, effective focal length f_e and one more parameter l in terms of the eccentricity ε .

$$l = \frac{2\varepsilon}{1 + \varepsilon^2}, \quad (1)$$

where ε changes with the type of reflective surface (Table 1). The entire catadioptric projection can be regarded as a nonlinear

* Project supported by the National Natural Science Foundation of China (No. 60502006, No. 60534070) and the Science and Technology Department of Zhejiang Province (No. 2007C21007).

transformation followed by a linear transformation, expressed in formula by six parameters as

$$\lambda \mathbf{m} = \mathbf{K} \mathbf{P} \mathbf{X}_s, \quad (2)$$

where λ is an unknown scalar.

	planar	ellipsoidal & hyperboloidal	paraboloidal
l	$l = 0$	$0 < l < 1$	$l = 1$

Table 1. mirror type and parameter l

3. CONSTRAINT ON A SET OF LINES

Without loss of generality, we study geometric properties of line image on metric plane Π_m , where $r = 1, s = 0, u_0 = 0$ and $v_0 = 0$.

In this section, we first derive the analytical expression of a line image in central catadioptric system using unifying model, and infer the properties of lines in terms of six parameters: aspect ratio r , skew factor s , principal point $\mathbf{O}_p (u_0, v_0)$, effective focal length f_e and l .

3.1 Projection of line

The generalized image formation of a line in space is shown in Figure 1. Line in 3D space is degenerately equivalent to the great circle on the unit sphere. A great circle is a circle defined by the intersection of the sphere and a plane passing through the origin [5]. Given a supporting plane $[n_x, n_y, n_z, 0]^T$, where $(n_x, n_y, n_z)^T$ is unit norm vector of the plane, hence the quadratic form of line image on metric plane Π_m is obtained [10]:

$$\mathbf{C} = \begin{pmatrix} (l^2 - 1)n_x^2 + l^2 n_z^2 & (l^2 - 1)n_x n_y & -f_e n_z n_x \\ (l^2 - 1)n_x n_y & (l^2 - 1)n_y^2 + l^2 n_z^2 & -f_e n_z n_y \\ -f_e n_z n_x & -f_e n_z n_y & -f_e^2 n_z^2 \end{pmatrix}. \quad (3)$$

By multiplying affine transformation \mathbf{K} , quadric form \mathbf{C}' of line image on image plane Π_M can be represented as:

$$\mathbf{C} = \mathbf{K}^T \mathbf{C}' \mathbf{K}^T, \quad (4)$$

where \mathbf{C} is conic on metric plane Π_m , and \mathbf{C}' is conic on plane Π_M .

3.2 Properties of a set of lines

Assume 3 great circles L_1, L_2, L_3 , which are projections of 3 space lines on unit sphere. Evidently if L_1, L_2, L_3 intersect at one point, they intersect the other antipodal point [7]. Note that, intersection points of lines in 3D space could be at infinity or not. Thanks to the nonambiguity of projection, it is indicated that parallel lines as well as a set of coplanar lines with a common point are suitable for practical calibration.

If a conic \mathbf{C} is the projection of a great circle on the metric plane Π_m , the projective contour from projection center \mathbf{O}_C is a cone. We get:

$$\mathbf{Q} = \mathbf{P}^T \mathbf{C} \mathbf{P} = \begin{pmatrix} af_e^2 & bf_e^2 & df_e & dlfe \\ bf_e^2 & cf_e^2 & ef_e & elfe \\ df_e & ef_e & f & fl \\ dlfe & elfe & fl & fl^2 \end{pmatrix}. \quad (5)$$

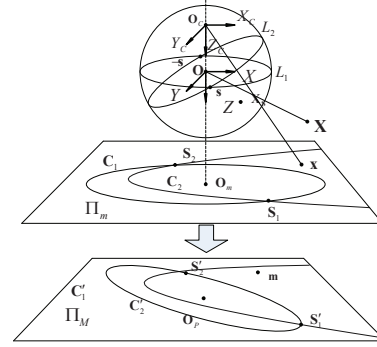


Figure 1. The unifying model for central catadioptric image formation.

Suppose there are a set of great circles intersected with two common antipodal points $\mathbf{s} = (s_x, s_y, s_z)^T$ and $-\mathbf{s}$ in homogeneous coordinate. Consequently, great circles correspond to a set of cones, whose common vertex is \mathbf{O}_C and two common generatrices are determined by \mathbf{s}, \mathbf{O}_C and $-\mathbf{s}, \mathbf{O}_C$ respectively. By representing the tangent plane Π_i using line coordinate

$$\Pi_i = \mathbf{Q}_i \mathbf{s} = \begin{bmatrix} a_i f_e^2 s_x + b_i f_e^2 s_y + d_i f_e s_z + d_i l f_e \\ b_i f_e^2 s_x + c_i f_e^2 s_y + e_i f_e s_z + e_i l f_e \\ d_i f_e s_x + e_i f_e s_y + f_i s_z + f_i l \\ d_i l f_e s_x + e_i l f_e s_y + f_i l s_z + f_i l^2 \end{bmatrix}, \quad (6)$$

we select first three factor of the normal vector at \mathbf{s} of cone \mathbf{Q}_i and note it as $\bar{\mathbf{n}}_i$. The direction of common generatrix is defined by the vector:

$$\bar{\mathbf{g}} = \bar{\mathbf{s}} - \bar{\mathbf{O}}_C = (s_x, s_y, s_y + l)^T. \quad (7)$$

Common generatrix is orthogonal to the normal vector of each cone at the corresponding common intersection point, which gives rise to a constraint.

Constraint. Common generatrix is orthogonal to each normal vector at the intersection point (shown in Figure 2)

$$\bar{\mathbf{n}}_i \bullet \bar{\mathbf{g}} = \begin{pmatrix} s_x \\ s_y \\ s_z + l \end{pmatrix}^T \begin{pmatrix} af_e^2 & bf_e^2 & df_e \\ bf_e^2 & cf_e^2 & ef_e \\ df_e & ef_e & f \end{pmatrix} \begin{pmatrix} s_x \\ s_y \\ s_z + l \end{pmatrix} = 0. \quad (8)$$

In next section, we expand the constraint from metric plane to image plane, and introduce algebraic distance in order to enhance the constraint of intersection.

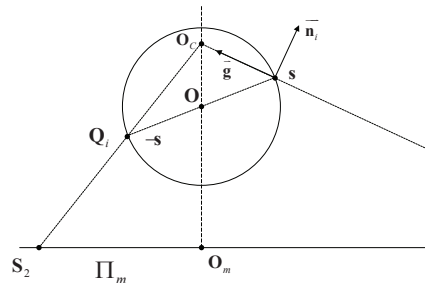


Figure 2. Conic section of a cone. \mathbf{s} and $-\mathbf{s}$ are two intersections on unit sphere. Vector $\bar{\mathbf{n}}_i$ is orthogonal to vector $\bar{\mathbf{g}}$. Dash lines indicate the degenerated conic section of projective cone from \mathbf{O}_C

4. CALIBRATION ALGORITHM

Intrinsic and external parameters compose the unknowns of conventional camera calibration. In this paper intrinsic parameters consist of aspect ratio, skew factor, principle point, focal length and the center of virtual camera. Only intrinsic parameters of central catadioptric system are involved in the proposed calibration algorithm other than external parameters.

Expanding the right side of (4), we get the constraint on intrinsic parameters and coefficients of conic on image plane:

$$\begin{cases} a = r^2 a' \\ b = r s a' + r b' \\ c = s^2 a' + 2 s b' + c' \\ d = r u_0 a' + r v_0 b' + r d' \\ e = s u_0 a' + u_0 b' + s v_0 b' + v_0 c' + s d' + e' \\ f = u_0^2 a' + 2 u_0 v_0 b' + v_0^2 c' + 2 u_0 d' + 2 v_0 e' + f' \end{cases} \quad (9)$$

Substituting \mathbf{s} with $(s_x, s_y, s_z)^T$ in (2), intersection point on image plane is obtained:

$$\mathbf{S}' = \begin{pmatrix} \frac{f_e s_x}{s_z \pm l} r + \frac{f_e s_y}{s_z \pm l} s + u_0, \frac{f_e s_y}{s_z \pm l} + v_0, 1 \end{pmatrix}^T. \quad (10)$$

Since Intersection point \mathbf{s} is a variable of 2 DOF, there are $2m+6$ unknowns considered in the proposed algorithm: $2m$ intersection points on m images, aspect ratio r , skew factor s , principal point (u_0, v_0) , effective focal length f_e , and one more parameter l .

So far, each line image provides one equation while there are 6 unknown intrinsic parameters to deal with. However, periodicity of trigonometric function makes minimization of constraint (8) to be a non-convex problem, where optimization algorithm will probably be trapped in local minimum. In order to enhance the constraint on image plane, we introduce **algebraic distance**, defined as:

$$D(\mathbf{C}', \mathbf{m}) = a'u^2 + 2b'uv + c'v^2 + 2d'u + 2e'v + f' = 0, \quad (11)$$

Any image of 2 line images, no matter whether they are parallel or not, will provide 6 independent equations, 3 for each line. 6 parameters can be sufficiently estimated by minimizing the 6 equations using nonlinear optimization algorithm such as Levenberg-Marquardt algorithm. The entire calibration algorithm could be written as:

$$\begin{cases} \min_{\mathbf{p}=\{r,s,u_0,v_0,f_e,l\}} (\bar{\mathbf{n}}_{ij} \cdot \bar{\mathbf{g}}_j) \\ \min_{\mathbf{p}=\{r,s,u_0,v_0,f_e,l\}} (D(\mathbf{C}'_{ij}, \mathbf{S}'_j)) \end{cases} \quad \text{where } i=1,2,\dots,n. j=1,2,\dots,m \quad (12)$$

where m stands for the amount of images, and n stands for the amount of lines in each image.

Initialization can be done by finding the boundary of mirror on image, and fitting an ellipse to the boundary. We use fitted ellipse of boundary to initialize ratio aspect, skew factor and principle point, whilst an invariant for line image to initialize

$$\text{focus length [10]: } r = \sqrt{-\frac{b'^2}{a'^2} + \frac{c'}{a'}} \quad , \quad s = -\frac{b'}{a'} \quad ,$$

$$u_0 = \frac{b'e' - c'd'}{a'c' - b'^2}, v_0 = \frac{b'd' - a'e'}{a'c' - b'^2}, f_e = \sqrt{-\frac{f_i(b_i f_i - d_i e_i)}{d_i(b_i d_i - a_i e_i)}}.$$

We get the normal vector for the supporting plane of great circle on the unit sphere: $\bar{\mathbf{n}}_i = (\cos \theta_i \sin \varphi_i, \sin \theta_i \sin \varphi_i, \cos \varphi_i)^T$.

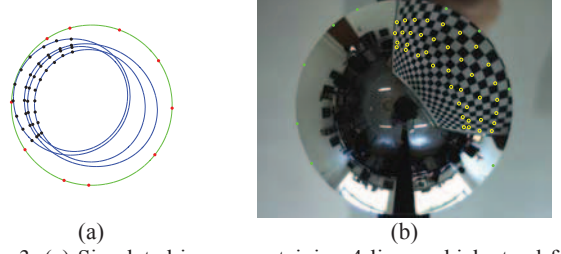


Figure 3. (a) Simulated image containing 4 lines, which stand for the planar grids, when Gaussian noise of deviation 2.0 pixels are added. Blue and green ellipses are estimated conics. (b) Real image with planar grids. Blue dots means manually extracted mirror boundary and yellow circles locate corners of chessboard.

From (3), the norm vector is derived by substituting f_e : $\theta_i = \arctan\left(\frac{e'_i}{d'_i}\right)$, $\varphi_i = \arctan\left(\frac{d'_i f_e}{f'_i \cos \theta_i}\right)$. Constructing a linear equation with a number of estimated normal vector $\mathbf{A}\mathbf{s} = 0$, where $\mathbf{A} = (\bar{\mathbf{n}}_1, \bar{\mathbf{n}}_2, \dots, \bar{\mathbf{n}}_i)^T$. If number of images is more than three, the solution to \mathbf{s} is the eigenvector of $\mathbf{A}^T \mathbf{A}$ with respect to the smallest eigenvalue. Otherwise, cross product of normal vectors $\mathbf{s} = \bar{\mathbf{n}}_1 \times \bar{\mathbf{n}}_2$ is conducted, if there are only 2 images.

5. EXPERIMENTS

This section states some experiments that demonstrate the performance of the proposed algorithm with simulation and real images. In principle, the calibration is absolutely accurate whenever conics corresponding to the line images are estimated without noise and quantization error. In practice, algorithm always suffers from inaccuracy of conic estimation and corner extraction. In these experiments, we make an assumption that l is a priori. According to the discussion in section 3.2, parallel lines are suitable in the proposed method. Taking practicality and convenience into consideration, we use chessboard of conventional camera calibration and manually label corners on the chessboard, while in simulated data, a set of points are simulated to imitate the chessboard.

5.1 Simulated Data

In simulation experiment, the central catadioptric system has the following parameters: $r = 1$, $s = 0$, $u_0 = 500$, $v_0 = 500$, $f_e = 300$. Image resolution is 1000×1000 , and we set $l = 0.9$ as a priori. From (3), projection of space line can be any type of conic when $l = 0.9$, for instance ellipse, circle, hyperbola, or parabola. Conic estimation plays a significant role in line-property-based calibration. Many conic estimation algorithms are presented in [11]. If $l^2 - 1 - n_z^2 > 0$, conic is an ellipse. We obtain that $0 \leq \varphi < 79.0472^\circ$. Considering the edge of the mirror, we chose $0 \leq \varphi < 20^\circ$ in the experiments. To simplify the experiment, we assume the line images are ellipse (or circle). Here, we use an ellipse-specific method called least squares fitting of ellipses [4].

Since the projection of the mirror boundary is manually selected in real data experiment, boundary in simulation is generated as shown in Figure 3. The simulated boundary is repres-

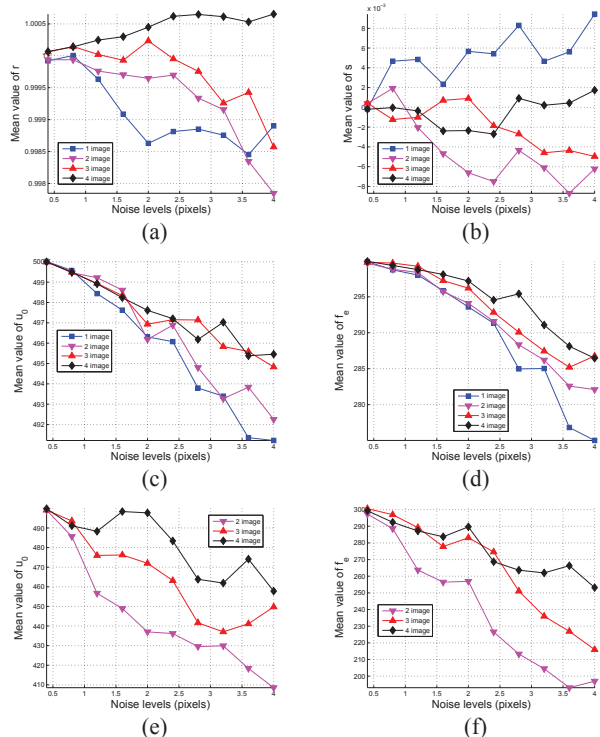


Figure 4. Results of simulation experiment. (a)(b)(c) and (d) for the proposed method. The performance of v_0 is similar to u_0 . (e) and (f) for the method proposed in [2]. The performance of r and s' is similar to those of the proposed method. Method in [2] can not apply this condition when all the conics have two common intersections. Hence, calibration with one image is not conducted in this method.

ented by 10 separated points randomly located along entire boundary. 4 lines compose the planar grids on each image with arbitrary orientation rotating about principle as well as vibration. On each projection curve we select 10 points with Gaussian noise of 0 mean and σ standard deviation. Deviation σ varies from 0 to 4.0 pixels with step of 0.4 pixels and the number of images varies from 1 to 4. For each noise level, the mean values of the parameters are calculated and 100 independent trials are conducted using Matlab. Experimental results are shown in Figure 4, while the results of the method proposed in [2] are shown for comparison. The results show that the proposed algorithm is robust in the condition of different noise levels. However, the results are not improved evidently by increasing the number of images. This might be attributed to the fitting inaccuracy of conics with low curvature, which influences the nonlinear optimization.

5.2. Real Data

The central catadioptric camera we used consists of hyperbolic mirror of eccentricity $\varepsilon = 1.3017$ and Sony XCD-SX910CR (<http://www.neovision.cz/prods/panoramic/h3s.html>). From (1), we get $l=0.9662$. The resolution of the image is 1280×960 . Conics and the mirror boundaries are extracted by labeling the corner of the chessboard and randomly selecting points on the

edge of the mirror respectively. The calibration results with real data are listed in Table 2.

Parameters	Results
r	$1.0002 \pm 9.7450 \times 10^{-5}$
s	$0.0147 \pm 4.5 \times 10^{-3}$
u_0	635.5244 ± 1.1578
v_0	480.2509 ± 1.1607
f_e	339.5925 ± 0.9399

Table 2. Calibration results with real data (using 4 images)

6. CONCLUSIONS

This paper introduces a novel constraint of lines that intersect on one or two (points at infinity) common points into central catadioptric camera calibration. It is proved that these lines could be parallel or concurrent and the minimum of two lines should be adequate for calibration in principle. We propose a calibration algorithm which parameterizes the intersection points and optimizes intrinsic parameters. The proposed algorithm requires commonly used planar grids, and corner points are manually selected as few as possible. In order to efficiently solve the non-linear equations, algebraic distance is applied to accelerate the convergence of Levenberg-Marquardt algorithm and enhance the intersection constrain against local minimum.

7. REFERENCE

- [1] S. Baker and S. Nayar. "A theory of catadioptric image formation". *Proc. Int'l Conf. Computer Vision*, pp. 35-42, 1998.
- [2] J. Barreto and H. Araujo, "Geometric Properties of Central Catadioptric Line Images," *Proc. Seventh European Conf. Computer Vision*, pp. 237-251, 2002.
- [3] J. Barreto and H. Araujo. "Geometric Properties of Central Catadioptric Line Images and Their Application in Calibration". *IEEE Trans. Pattern Analysis and Machine Intelligence*, vol. 27, no. 8, pp. 1327-1333, Aug. 2005.
- [4] A. Fitzgibbon, M. Pilu, and R. Fisher, "Direct Least Square Fitting of Ellipses," *IEEE Trans. Pattern Analysis and Machine Intelligence*, vol. 21, no. 5, pp. 476-480, May 1999.
- [5] C. Geyer and K. Daniilidis, "An Unifying Theory for Central Panoramic Systems and Pratical Implications," *Proc. European Conf. Computer Vision*, pp. 445-461, 2000.
- [6] D. Scaramuzza1, A. Martinelli, R. Siegwart. "A Flexible Technique for Accurate Omnidirectional Camera Calibration and Structure from Motion". *Proc. Int'l Conf. ICVS*, pp. 45, 2006.
- [7] T. Svoboda, T. Padjla, and V. Hlavac, "Epipolar Geometry for Panoramic Cameras," *Int'l J. Computer Vision*, vol. 49, no. 1, pp. 23-37, 2002.
- [8] R. Swaminathan, M. D. Grossberg and S. K. Nayar. "Caustics of Catadioptric Cameras". *Proc. Int'l Conf. Computer Vision*, pp. 2-9, 2001.
- [9] J-P. Tardif, P. Sturm, S. Roy. "Plane-based self-calibration of radial distortion". *Proc. Eleventh Int'l Conf. Computer Vision*, pp. 1-8, 2007.
- [10] X. Ying and Z. Hu, "Catadioptric Camera Calibration Using Geometric Invariants," *IEEE Trans. Pattern Analysis and Machine Intelligence*, vol. 26, no. 10, pp. 1260-1271, Oct. 2004.
- [11] Z. Zhang, "Parameter Estimation Techniques: A Tutorial with Application to Conic Fitting," *INRIA Rapport de Recherche* n 2676, Oct. 1995.